

pubs.acs.org/JACS Article

Layered and Cubic Semiconductors $AGaM'Q_4$ ($A^+ = K^+$, Rb^+ , Cs^+ , Tl^+ ; $M'^{4+} = Ge^{4+}$, Sn^{4+} ; $Q^{2-} = S^{2-}$, Se^{2-}) and High Third-Harmonic Generation

Daniel Friedrich, Hye Ryung Byun, Shiqiang Hao, Shane Patel, Chris Wolverton, Joon Ik Jang, and Mercouri G. Kanatzidis*



Cite This: J. Am. Chem. Soc. 2020, 142, 17730-17742



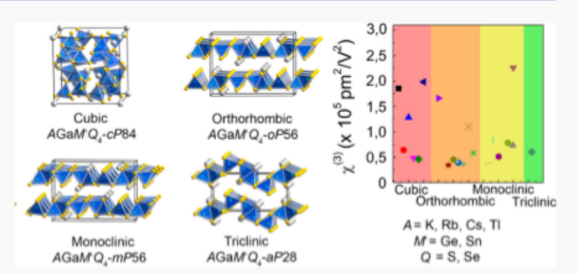
ACCESS |

III Metrics & More

Article Recommendations

Supporting Information

ABSTRACT: Eighteen new quaternary chalcogenides $AGaM'Q_4$ ($A^+ = K^+$, Rb^+ , Cs^+ , Tl^+ ; $M'^{4+} = Ge^{4+}$, Sn^{4+} ; $Q^{2-} = S^{2-}$, Se^{2-}) have been prepared by solid-state syntheses and structurally characterized using single-crystal X-ray diffraction techniques. These new phases crystallize in a variety of layered structure types. The tin analogues also adopt an extended three-dimensional network structure as polymorphs. The polymorphism and phase-stability in these cases were studied by thermal analysis and high-temperature in situ X-ray powder diffraction. All compounds are semiconductors with the colored selenides absorbing light in the infrared-green region (1.8 eV < $E_{\rm g}$ < 2.3 eV) and the mostly white



sulfides absorbing light in the blue-ultraviolet range (2.5 eV < $E_{\rm g}$ < 3.6 eV). Based on third-harmonic generation (THG) measurements, the third-order nonlinear optical (NLO) susceptibilities $\chi^{(3)}$ of the new and previously reported $AGaM'Q_4$ compounds were determined. These measurements revealed an apparent correlation between the THG response of the sample and its band gap, rather than the crystal structure type. While low-gap materials possess higher nonlinearity in general, we found that layered orthorhombic RbGaGeS₄ exhibits an impressive $\chi^{(3)}$ value (about four times larger than that of AgGaS₂) even with a large band gap and shows stability under ambient conditions with no significant irradiation damage.

■ INTRODUCTION

Quaternary chalcogenide compounds $A_a M_b M'_c Q_d$ (A = alkali metal, thallium; M, M' = transition or main group metal; Q = chalcogen) are an interesting class of solids with a large variety of stoichiometric compositions and structures. Quaternary compounds $A_a M_b M'_c Q_d$ (A = alkali metal, thallium; M = group 13 metal; M' = group 14 metal; Q = chalcogen) promise to deliver broad sets of chemical and physical functions depending on their structure types and compositions. Examples include the fast ion exchange in KInSn₂S₆¹ for the capture of lanthanide ions and the strong nonlinear optical (NLO) second-harmonic generation (SHG) of noncentrosymmetric compounds. Materials like LiGaGe₂ Q_6 , $^{2-5}$ A_2 In₂ $M'Q_6$, $^{6-9}$ and TlGaSn₂ Q_6 are especially promising NLO candidates. For the compounds with the stoichiometric composition $AMM'Q_4$ (A = K, Rb, Cs, Tl; M = Al; Ga, In; M'= Si; Ge, Sn; Q = S, Se), compounds containing indium and mixtures of gallium and tin have been mostly reported. 14-22 Among the respective gallium germanium compounds only KGaGeS₄ has been reported.²⁰ The present work deals with the discovery, structural characterization, and optical properties of a series of new gallium compounds $AGaM'Q_4$ (A = K, Rb, Cs, Tl; M' = Ge, Sn; Q = S, Se). In the course of our work we successfully managed to prepare and structurally characterize new compositions in these systems. Furthermore, we also

discovered new crystalline polymorphs. For the quaternary gallium chalcogenides, different dimensionalities of the crystal structures are observed. The lighter gallium germanium phases solely crystallize as layered compounds with varying symmetry and different polymorphs. CsGaGeS₄ for example crystallizes in three different two-dimensional (2D) layered structures. For the heavier gallium tin compounds, such two-dimensional structures are also observed. However, these phases appear to also be stable in a three-dimensional (3D) network structure depending on the syntheses conditions.

We characterized the optical properties of our new materials using UV/vis optical spectroscopy and first-principles quantum chemical density functional theory (DFT) calculations. Our results revealed that all these compounds are semiconductors with the colored selenides absorbing light in the infrared (IR)-green region (1.8 eV $< E_{\rm g} < 2.3$ eV) and the mostly white sulfides absorbing light in the blue-ultraviolet (UV) range (2.5

Received: August 11, 2020 Published: September 15, 2020





 $eV < E_{\alpha} < 3.6 eV$). As all isolated phases are centrosymmetric solids, they have no SHG properties. While studies of SHG in the context of the crystal structure has been of interest for many years, the study of third-harmonic generation (THG) is relatively rare in the literature and the corresponding database of such properties is small. Therefore, unlike the case with SHG materials, it is difficult to develop an intuitive understanding of structure/property relationships with response to THG. As a set, these iso-stoichiometric compounds present an opportunity to study the NLO properties in such a context. Since THG occurs in all materials regardless of their symmetry, we therefore investigated these compounds regarding their third-order NLO properties. Here, we measured THG and assessed the third-order nonlinearity $\chi^{(3)}$ of powdered samples.^{23,24} We found that several title compounds possess large third-order susceptibilities that exceed the $\chi^{(3)}$ values of the reference materials, AgGaS₂ or AgGaSe2. Furthermore, a trend of increasing nonlinearity with a decrease of the optical band gap is observed in the AGaM'Q4 compounds, independent of the crystal structure. Intriguingly, however, we found that RbGaGeS4 is an outlier, possessing a high THG response and a large band gap at the same time. Our results show that these compounds are promising for third-order NLO applications that rely on nonlinear refractive index and two-photon absorption.²⁵

■ EXPERIMENTAL SECTION

Starting Materials. Commercially available chemicals potassium (K, Sigma-Aldrich, 99.95%), rubidium (Rb, Alfa Aesar, 99.5%), cesium (Cs, Alfa Aesar, 99.5%), thallium (Tl, Alfa Aesar, 99.99%) gallium (Ga, SNMET, 99.99%), germanium (Ge, American Elements, 99.99%), tin (Sn, American Elements, 99.99%), sulfur (S, SN Plus, 99.99%), and selenium (Se, American Elements, 99.999%) were used without further purification. The A_2Q (A = K, Rb, Cs; Q = S, Se) were prepared by reaction of the alkali metals with the respective chalcogens in liquid ammonia. Gallium chalcogenides were prepared by reaction of Ga and the respective chalcogen at 1000 °C (Ga_2S_3) and 600 °C (Ga_2Se_3), respectively. GeS_2 and SnS_2 were prepared by annealing of the elements at 800 and 550 °C, respectively.

Synthesis of the Title Compounds. All quaternary compounds were prepared by high-temperature reaction of stoichiometric amounts of the respective starting materials in flame-sealed and evacuated fused silica tubes. In a typical reaction batch of 1.0 g, stoichiometric amounts of alkali metal chalcogenides A2Q combined with the other precursor materials were weighed in a fused silica tube (inner diameter 8 mm) in a nitrogen-filled glovebox. The tubes were evacuated to $\sim 10^{-4}$ mbar and flame-sealed. The $\sim 10-11$ cm long tubes were placed in a programmable furnace and annealed according to the respective heating programs. The full details on the syntheses and temperature programs can be found in the Supporting Information. After opening of the tubes, phase-purity and crystallinity of the resulting materials were determined by X-ray powder diffraction techniques. Unless otherwise noted, all samples are single-phase solids. X-ray powder diffraction patterns of all new phases that could be produced in larger bulk quantities are shown in the Supporting Information (Figures S1-S4). A general rule for the synthesis of these AGaM'Q4 compounds seems that the layered 2D polymorphs only form at high temperatures or after cooling of a molten batch, while the 3D network compounds need to be annealed for an extended amount of time below the melting point. All sulfide compounds are stable in moist air, while the selenides decompose within several minutes by releasing gaseous H₂Se and turning black. The samples were therefore stored in a glovebox and only exposed to air for minimal time before any characterization.

Single Crystal X-ray Diffraction. Suitable single crystals of the title compounds were selected under a microscope and fixed to

MiTeGen mounts using silicon grease. Diffraction data was collected at ambient temperatures on a Bruker Kappa APEX II diffractometer equipped with an I μ S microfocus X-ray (Mo K α radiation, λ = 0.71073 Å) source and an APEX2 CCD detector. The resulting diffraction data were corrected for Lorentz and polarization effects, and absorption was corrected by a numerical absorption correction (based on the crystal faces) using the Bruker APEX II software suite. All data sets had a completeness of 99.9% within 50° 2 θ . The crystal structures were solved by intrinsic phasing methods using ShelXT2018/3 and refined on F^2 with ShelXL2018/3 using full-matrix least-squares methods.

Further details on the crystal structure investigations may be obtained from the Fachinformationszentrum Karlsruhe, 76344 Eggenstein-Leopoldshafen, Germany, on quoting the depository numbers CSD-2018860 for RbGaGeS₄ (1), CSD-2018859 for RbGaGeSe₄ (2), CSD-2018866 for TlGaGeS₄ (3), CSD-2018863 for TlGaGeSe₄-oP56 (4), CSD-2018857 for CsGaGeS₄-oP56 (5), CSD-2018862 for CsGaGeSe₄ (6), CSD-2018854 for CsGaSnS₄-oP56 (7), CSD-2018855 for KGaGeSe₄ (8), CSD-2018869 for TlGaSnS₄mP56 (9), CSD-2018867 for TlGaSnSe₄-mP56 (10), CSD-2018861 for TlGaGeSe₄-mC112 (11), CSD-2018853 for CsGaGeS₄-mP28 (12), CSD-2018852 for CsGaGeS₄-aP28 (13), CSD-2018856 for KGaSnSe₄-cP84 (14), CSD-2018858 for RbGaSnSe₄-cP84 (15), CSD-2018865 for TlGaSnS₄-cP84 (16), CSD-2018868 for TlGaSnSe₄-cP84 (17), and CSD-2018864 for CsGaSnS₄-cP84 (18). All compounds presented in this work have mixed occupation of the Ga3+ and M4+ cations on all respective sites. For a charge balanced compound, the ideal ratio of Ga^{3+}/M^{4+} in all compounds has to be 1:1. Therefore, all initial structure refinements were performed under the assumption of equal occupancy of Ga3+ and Ge4+ or Sn4+, respectively. For the layered mixed Ga3+/Sn4+ compounds, however, large low electron density maxima on the difference Fourier map and large R values were obtained after the initial refinement. In order to properly treat the mixed occupation, all metal occupation factors were freely refined. The resulting structure models converged in all cases with a total Ga3+/M4+ ratio of 1:1. As we wanted to treat the mixed Ga3+/Sn4+ occupation with the least amount of restrictions possible, the occupation factors in these structures were refined using free variables for all sites. All sites in the Ga3+/Ge4+ compounds were kept at 50% occupancy for both cations as they cannot be properly distinguished using conventional single-crystal X-ray techniques. For the alkali metal compounds, all refinements converged with a perfect 1:1 ratio of Ga^{3+} and Sn^{4+} and full occupancy of all A^{+} and Q^{2-} sites. Additional constraints in the form of a SUMP command were therefore not necessary. All layered thallium compounds show a severe disorder on all Tl+ sites, which was treated by splitting the site in two new sites and free refinement of the occupation factors using another free variable to ensure charge balance. The structural refinement of the compound labeled TlGaGeSe4-mC112 revealed that this phase is in fact not an ideal AMM'Q4 compound as its stoichiometry converged with the sum formula Tl_{0.8}Ga_{0.8}Ge_{1.2}Se₄ and one not fully occupied TI+ site. For this compound, the occupation factors of TI+, Ga5+, and Ge4+ were also constraint using a SUMP

X-ray Powder Diffraction. X-ray powder diffraction patterns were collected on a Rigaku Miniflex600 diffractometer using $Cu-K\alpha 1$ radiation ($\lambda=1.540593$ Å) equipped with a high-speed silicon strip detector. Finely powdered samples were measured on a flat zero-background Si sample. The experimental patterns were compared to simulated patterns based on the experimental CIF files.

In Situ High-Temperature X-ray Powder Diffraction. For the high-temperature X-ray diffraction experiments, powdered samples were flame-sealed in evacuated fused silica capillaries (diameter 0.3 mm). The samples were measured on a STOE Stadi P diffractometer equipped with a Dectris Mythen 1K detector using monochromatic Mo–K α 1 radiation (λ = 0.70930 Å). The samples were heated by a STOE high-temperature capillary furnace. The WinXPOW software package from STOE & Cie was used for data collection and processing.

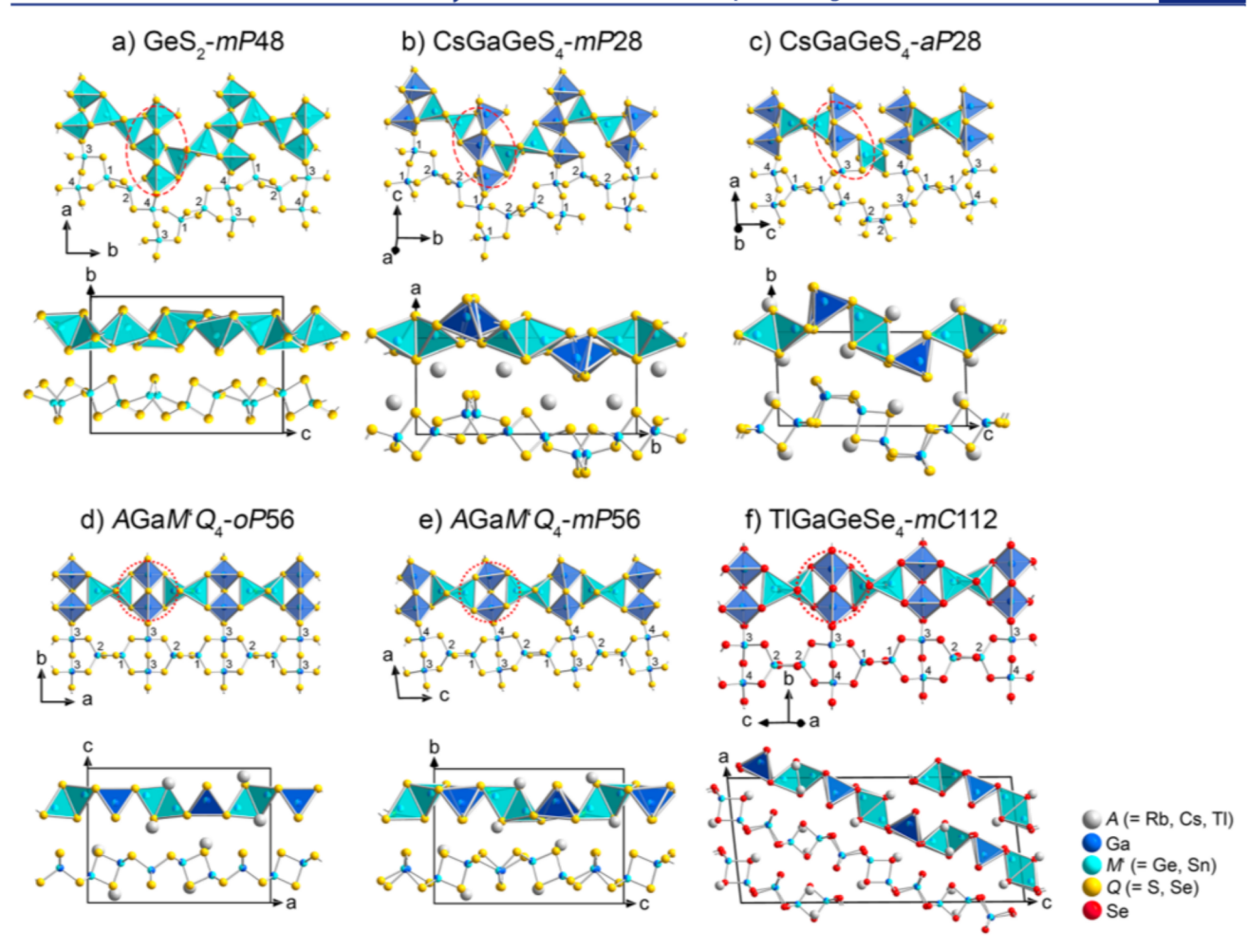


Figure 1. Crystal structures and sections of the anionic substructures of the layered $AGaM'Q_4$ phases (b-f) and their related structure GeS_2 -mP48 (a). The mixed Ga/M' cation sites are labeled and the difference in the linkage of the atoms in the layers is highlighted by the dashed and dotted red circles, respectively.

UV/vis Diffuse Reflectance Spectroscopy. The diffuse-reflectance measurements were performed at room temperature using a Shimadzu UV-3101 PC double-beam, double-monochromator spectrometer. $BaSO_4$ was used as a white standard (100% reflectance) and spectra were collected in the range of 200–2500 nm with a resolution of 2 nm. The absorption spectra were calculated from the raw data using the Kubelka–Munk equation. 27

Differential Thermal Analysis. For the differential thermal analysis, powdered samples (\sim 25 mg) were flame-sealed in fused silica ampules. The measurements were performed on a Netzsch STA F3 Jupiter operating in thermogravimetric analysis-DTA mode. Two heating and cooling cycles of all samples were collected with heating and cooling rates of 10 °C/min. A similarly prepared $\rm Al_2O_3$ sample was used as a reference material.

Density Functional Theory (DFT) Calculations. DFT calculations within the generalized gradient approximation (GGA) were used to calculate electronic structures of the title compounds. The Perdew—Burke—Ernzerhof exchange correlation functional with Projector Augmented Wave potentials were applied to all calculations. The periodic boundary conditions and a plane-wave basis set were utilized as implemented in the Vienna ab initio simulation package. The total energies were numerically converged to approximately 3 meV/cation using a basis set energy cutoff of 500 eV and dense k-meshes corresponding to 4000 k-points per reciprocal atom in the Brillouin zone. In order to find proper structure models for the mixed Ga³⁺/M'⁴⁺ occupation, the lowest energy configuration was chosen from a vast number of geometrically distinct Ga³⁺/M'⁴⁺

possibilities. For the 10 structures with the lowest electrostatic energies, further DFT calculations were performed to identify the most favorable (lowest energy) configuration.

Third-Harmonic Generation (THG) Measurements. The phase-matching (PM) behavior of the title compounds was investigated using polycrystalline powdered samples. For each compound, six fractions of different grain sizes (25–32, 32–45, 45–62, 62–90, 90–106, and 106–150 μ m) were prepared by mechanical sieving of the finely grounded powders. Each sample was flame-sealed in a glass capillary (diameter 1 mm) to prevent moisture and air exposure, and mounted on a homemade sample holder. The THG efficiencies of the samples with wide (narrow) bandgaps were compared with a reference material AgGaS₂ (AgGaSe₂).

The THG measurements were carried out at room temperature using input wavelengths of $\lambda=1800$ and 2400 nm, respectively, for wide-gap and narrow-gap compounds with an intensity of 2.74 GW/cm². This intensity did not result in any significant irradiation damage. Coherent light with a wavelength of 1064 nm was initially produced using an EKSPLA PL-2250 series diode-pumped Nd:YAG laser with a pulse width of 30 ps and a repetition rate of 50 Hz to generate tunable pulses. The Nd:YAG laser pumped an EKSPLA Harmonics Unit (HU) H400, in which the input beam was frequency tripled by a sum frequency generation scheme. The beam then entered an EKSPLA PG403-SH-DFG Optical Parametric Oscillator (OPO) composed of four main parts: (i) a double-pass parametric generator, (ii) a single pass parametric amplifier, (iii) a second-harmonic generator (SH), and (iv) a difference frequency generation (DFG) scheme. The

Table 1. Crystallographic Data of the Orthorhombic Layered AGaM'Q4 Compounds

	RbGaGeS ₄ (1)	RbGaGeSe ₄ (2)	TlGaGeS ₄ (3)	TlGaGeSe ₄ -oP56 (4)	$CsGaGeS_{4}$ - $oP56$ (5)	CsGaGeSe ₄ (6)	$CsGaSnS_{4}$ - $oP56$ (7)			
space group	Pnma (no. 60)									
a/Å	16.8539(6)	17.5750(5)	16.7942(5)	17.4742(4)	17.0125(8)	17.7666(7)	17.5708(5)			
b/Å	7.1330(3)	7.4718(2)	7.1027(2)	7.4105(2)	7.1848(3)	7.5171(3)	7.3846(2)			
c/Å	12.1410(5)	12.4449(4)	11.5193(4)	11.9406(3)	12.5038(6)	12.6383(5)	12.4343(3)			
$V/Å^3$	1459.6(1)	1634.2(1)	1374.07(7)	1546.2(1)	1528.4(1)	1687.9(1)	1613.4(1)			
Z	8									
$ ho_{ m calc}/{ m g\cdot cm^{-3}}$	3.240	4.419	4.564	5.692	3.507	4.652	3.699			
$\mu(\text{Mo }K\alpha)/\text{mm}^{-1}$	15.461	30.605	32.404	46.834	13.132	28.154	11.812			
T/°C	20									
$R_{\rm int}$ R_{σ}	0.0620, 0.0182	0.0465, 0.0136	0.0415, 0.0209	0.0482, 0.0231	0.0513, 0.0157	0.0562, 0.0184	0.0303, 0.0569			
R_1 , wR_2 $[I > 3\sigma(I)]$	0.0206, 0.0499	0.0139, 0.0282	0.0199, 0.0383	0.0238, 0.0579	0.0154, 0.0306	0.0152, 0.0344	0.0191, 0.0447			
R_1 , wR_2 [all data]	0.0258, 0.0519	0.0187, 0.0292	0.0270, 0.0406	0.0294, 0.0604	0.0190, 0.0316	0.0168, 0.0348	0.0209, 0.0460			
$\Delta ho_{ m min}$, $\Delta ho_{ m max}$ /e-Å $^{-3}$	-0.537,0.622	-0.503, 0.571	-1.154, 1.314	-1.671, 1.768	-0.509, 0.709	-0.680,0.552	-0.762,0.849			

^aThe full details of the data collection and structural refinement can be found in the Supporting Information.

output wavelengths of the OPO used in our experiments were 1800 and 2400 nm. These wavelengths were deliberately selected in order to make sure that THG (600 and 800 nm) occurs below the bandgap of both test samples and reference materials. This implies that the effect of multiphoton absorption can be neglected in our measurements, and therefore, THG arises mostly from the real part of the third-order nonlinearity. The THG signal was collected using a reflection geometry and a fiber-optic bundle coupled to a spectrometer (Horiba iHR320) equipped with a CCD camera (Horiba Synapse). The data collection time was 450 s.

RESULTS AND DISCUSSION

Prior to this work, KGaGeS₄ 20 and a series of AGaSn Q_4 (A = K, Rb, Tl, Cs; Q = S, Se) 16,17,19,20,30 compounds were the only reported quaternary compounds with the stoichiometric composition AGa $M'Q_4$ (M' = Ge, Sn) in the literature. In this work we successfully prepared all previously unknown combinations and in some cases discovered new crystalline polymorphs. As most quaternary compounds reported in this work crystallize in more than one crystalline modification or represent a new polymorph of an already known composition, in order to distinguish these polymorphs, we added the Pearson symbol (e.g., -oP56, -mP56, and -cP84) at the end of the sum formula as a unique identifier as suggested by the IUPAC and IUCr. The symbols indicate the crystal system, lattice centering, and number of atoms per unit cell, respectively.

Crystal Structure Description. Due to the large amount of structures and structure types, only the most important aspects of the crystal structures of the new compounds will be discussed here. Further crystal structure data and interatomic distances are listed in the Supporting Information (Tables S1–S72).

The $AGaM'Q_4$ (A = K, Rb, Cs; M' = Ge, Sn; Q = S, Se) compounds form plate-shaped crystals and crystallize in 2D layered structures. The structure of the layers found in these compounds is related to the high-temperature modification of GeS_2 (in this work called GeS_2 -mP48). In order to better understand the layered structures it is best to break them into different building units and to describe the layers as being composed of condensed corner-sharing tetrahedra chains linked by edge-sharing Ge_2S_6 double tetrahedra units perpendicular to the chain direction. Each Ge_2S_6 linker is connected to two consecutive tetrahedra in the chains by four common corners (Figure 1a). In GeS_2 -mP48, the Ge^{4+} cations occupy four crystallographically independent

atomic sites with two each located in the corner-sharing chain and the double tetrahedra. For reasons of consistency, the sites forming the M_2Q_6 linkers (M = Ga/Ge, Ga/Sn) are referred to as M1 and M2, and the sites of the corner-sharing tetrahedra chain are labeled M3 and M4 for all layered polymorphs in this work (site labels can be found in Figure 1). The only exception to this labeling scheme is monoclinic CsGaGeS₄-mP28 which only has two M sites, thus making M2 the linker site.

The substitution of half of the $\mathrm{Ge^{4^+}}$ cations with $\mathrm{Ga^{3^+}}$ cations in these layers, creates anionic layers $_\infty^2[\mathrm{GaGeS_4}^-]$. In order to preserve charge balance, alkali metal counter cations fill the voids in and between the anionic layers. The specific combination of the elements also influences the symmetry of the resulting structure with the higher symmetry orthorhombic polymorphs exhibiting the most regular layers, compared to the lower symmetry monoclinic and triclinic polymorphs. The crystal structures of the different layered $\mathrm{AGaM'Q_4}$ polymorphs are discussed in more detail below.

The monoclinic polymorph CsGaGaS₄-mP28 (12) crystal-lizes in the space group $P2_1/c$ and is isotypic to the known compound KGaGeS₄- $^{2.0}$ The structure of this compound is closely related to GeS₂-mP48 as it retains an identical connectivity of the atoms in the anionic layers. Furthermore, the unit cell parameters of the solid and its parent structure are very similar to GeS₂-mP48 having an axis along the layers doubled and a different monoclinic angle. These differences likely result from the incorporation of the alkali metal cations A^+ in between the anionic layers, causing a distortion in the structure. Consequently, the anionic layers in CsGaGeS₄-mP28 have a slightly more distorted shape than GeS₂ layers due to the cations widening the gap between the layers.

A triclinic polymorph of CsGaGeS₄, CsGaGaS₄-aP28 (13), crystallizes in the triclinic space group $P\overline{1}$ isotypic to the known compounds KGaSnS₄ and KInGeS₄. The anionic substructure of this phase retains the ${}_{\infty}^{2}$ [GaGeS₄- ${}_{1}$] layers found in CsGaGeS₄-mP28 and GeS₂-mP48. The lower symmetry of the structure, however, results in a significant distortion of the layers giving them a "wavy" look (Figure 1) when viewed parallel to the layers. Interestingly, the Cs⁺ cations in this phase are also 9-fold coordinated by the S²⁻ anions like in CsGaGeS₄-mP28, and the mean distances \overline{d} (Ga/Ge-S) are basically identical. The main structural difference between CsGaGaS₄-aP28 and its monoclinic polymorph is that, in monoclinic CsGaGaS₄-mP28, the anionic layers are completely

Table 2. Crystallographic Data of the Monoclinic and Triclinic Layered AGaM' Q4 Compounds

	KGaGeSe ₄ (8)	$TlGaSnS_{4}-mP56$ (9)	TlGaSnSe ₄ -mP56 (10)	TlGaGeSe ₄ -mC112 (11)	CsGaGeS ₄ -mP28 (12)	CsGaGeS ₄ -aP28 (13)
space group		$P2_1/c$ (no. 14)		C2/c (no. 15)	$P2_1/c$ (no 14)	P1 (no. 2)
a/Å	7.3552(2)	7.2516(2)	7.501(1)	13.5831(4)	7.6995(5)	7.1611(1)
b/Å	12.4151(3)	11.6629(4)	12.175(1)	7.4015(2)	16.3721(9)	7.5944(2)
c/Å	17.6213(4)	17.5044(5)	18.203(1)	30.7410(7)	6.8930(4)	14.6345(3)
α/deg	90	90	90	90	90	91.003(2)
β/\deg	97.026(2)	95.267(3)	97.164(3)	96.066(2)	111.894(4)	92.314(2)
γ/deg	90	90	90	90	90	106.680(2)
$V/\mathrm{\AA}^3$	1597.02(7)	1474.18(8)	1649.4(2)	3073.3(1)	806.24(9)	761.42(3)
Z		8		16	4	4
$ ho_{ m calc}/{ m g\cdot cm^{-3}}$	4.136	4.695	5.646	5.379	3.324	3.520
$\mu(\text{Mo K}\alpha)/\text{mm}^{-1}$	25.783	29.813	42.329	43.032	12.447	13.180
T/°C				20		
R_{int} R_{σ}	0.0534, 0.0407	0.0503, 0.0311	0.0442, 0.0253	0.0446, 0.0265	0.0528, 0.0239	0.0393, 0.0222
R_1 , wR_2 $[I > 3\sigma(I)]$	0.0257, 0.0458	0.0458, 0.1148	0.0358, 0.0853	0.0293, 0.0689	0.0231, 0.0572	0.0170, 0.0414
R_1 , wR_2 [all data]	0.0439, 0.0499	0.0523, 0.1178	0.0434, 0.0887	0.0328, 0.0700	0.0277, 0.0603	0.0182, 0.0419
$\Delta ho_{ m min}$ $\Delta ho_{ m max}$ /e-Å $^{-3}$	-0.662, 0.669	-1.710, 1.961	-1.758, 2.642	-1.243, 1.186	-1.259, 0.910	-0.631, 0.799

[&]quot;The full details of the data collection and structural refinement can be found in the Supporting Information.

separated by the Cs⁺ cations, while in the triclinic structure the Cs⁺ cations are closer to the layers.

Because of the increased symmetry (orthorhombic, space group Pnma) in the mixed Ga/Ge compounds RbGaGeS₄ (1), RbGaGeSe₄ (2), TlGaGeS₄ (3), TlGaGeSe₄-oP56 (4), CsGaGeSe₄ (5), CsGaGeS₄-oP56 (6), and CsGaSnS₄-oP56 (7), a slight change in the layered structure occurs. Basic crystallographic data for these compounds can be found in Table 1. The same structure was also reported for the analogous $AMM'Q_4$ compounds $CsInGeQ_4$ $(Q = S, Se)^{14,16}$ and CsGaSnSe₄. 19 At first glance, the $_{\infty}^{2}$ [GaM'Q $_{4}^{-}$] layers in the ab plane in this structure appear identical to the monoclinic layers found in GeS₂-mP48 and related compounds. The main difference of these layers to the GeS2-mP48 type layers is the arrangement of the M2Q6 linkers, which are staggered in the GeS2-mP48 type layers and aligned perfectly straight along the crystallographic a axis in the orthorhombic structures. Ga3+ and M4+ cations occupy only three crystallographically independent sites compared to the four in GeS2 with Ga/ M'1 and Ga/M'2 on special sites forming the Ga_2Q_6 linkers and the Ga/M'3 site solely forming the linear chains (site labels see Figure 1). The higher symmetry sites lead to an overall less distorted appearance of the anionic layers compared to monoclinic GeS₂. The A^+ cations (A = Rb, Cs, Tl) found in the voids in-between the anionic layers occupy two crystallographically independent sites. Both sites are 9-fold (7 + 2) coordinated by the chalcogenide anions within a sphere of 4.2 Å.

The compounds KGaGeSe₄ (8), TlGaSnS₄-mP56 (9), and TlGaSnSe₄-mP56 (10) and the previously reported compounds KGaSnSe₄, ¹⁹ RbGaSnSe-mP56, ³⁰ and KInSnSe₄, ¹⁸ crystallize in a 2D layered structure in the monoclinic space group $P2_1/c$. Basic crystallographic data for these compounds can be found in Table 2. This structure type, however, differs from GeS₂-mP48 layers in the same way as the orthorhombic layers by the arrangement of the M_2Q_6 linkers in the layers. This structure is basically a lower symmetry version of the orthorhombic $AMM'Q_4$ -oP56 compounds with the Ga³⁺ and M'^{4+} cations occupying four crystallographically independent common sites. Consequently, the layers exhibit a slight distortion compared to the orthorhombic polymorphs.

In the batch of TlGaGeSe₄-oP56, a few single crystals of a different, monoclinic C-centered phase could be isolated. A free refinement of the crystal structure immediately revealed that the sum formula for this phase is "Tl_{0.8}Ga_{0.8}Ge_{1.2}Se₄" (11). As the crystal structure is still related to the other phases and in order to distinguish this phase from orthorhombic TlGaGeSe₄-oP56, it will be labeled "TlGaGeSe₄"-mC112. The anionic layers $_{\infty}^{2}$ [GaGeS₄] in this compound run parallel to the (101) direction and have a slight distortion similar to the other monoclinic phases like TlGaSnQ₄-mP56 (Figure 1). All interatomic distances in both TlGaGeSe₄ polymorphs are basically identical. Both Tl† sites in TlGaGeSe₄-mC112 are 9-fold coordinated by Se²-within 4.0 Å.

For all layered polymorphs of the AGaM'Q4 compounds and related phases, the observed mean distances $\overline{d}(Ga/M'-Q)$ are basically identical for a given combination of elements with values of $\overline{d}(Ga/Ge-S) \approx 2.24(1) \text{ Å}, \overline{d}(Ga/Sn-S) \approx 2.34(1)$ Å, $\overline{d}(Ga/Ge-Se) \approx 2.38(1)$ Å, and $\overline{d}(Ga/Sn-Se) \approx 2.46(1)$ A. Very minor variances can be attributed to slight influence of different A+ cations. These values are also in good agreement with the sum of the ionic radii d(Ga-S) = 2.31 Å, d(Ge-S) =2.23 Å, d(Sn-S) = 2.39 Å, d(Ga-Se) = 2.45 Å, d(Ge-Se) =2.37 Å, and $d(Sn-Se) = 2.53 Å.^{33}$ The distances d(Ga/M'-Q)in the Ga/M'Q4 tetrahedra vary with the connectivity of the tetrahedra among each other. In the edge-sharing $(Ga/M')_2Q_6$ linker, the distances d(Ga/M'-Q) are slightly shorter due to the edge-sharing and each tetrahedron only being connected to three adjacent tetrahedra. The distances d(Ga/M'-Q) observed in the corner-sharing tetrahedra which are linked to four neighbors are slightly longer. Consequently, the distances d(Ga/M'-Ga/M') in these tetrahedra also vary with the connectivity of the tetrahedra and shorter distances d(Ga/M'-Ga/M') are observed in the edge-sharing linkers. In all layered polymorphs, all A⁺ cation sites are 9-fold coordinated by Q²⁻ anions within a sphere of ~4.2 Å. The resulting polyhedra cannot be attributed to a regular coordination polyhedron. In the monoclinic polymorphs AGaM'Q4-mP56, this 9-fold coordination is more akin to a 7 + 2 fold coordination with seven shorter distances d(A-Q) < 4 Å and two slightly longer distances 4 Å < d(A-Q) < 4.2 Å. All the observed distances in these compounds are in good agreement with already known $AMM'Q_4$ compounds 20,22,31 and binary and ternary gal-